

Article

Formation of Aligned α -Si₃N₄ Microfibers by Plasma Nitridation of Si (110) Substrate Coated with SiO₂

Chang-Hua Yu ^{1,*}, Kun-An Chiu ¹, Thi-Hien Do ¹, Li Chang ^{1,*} and Wei-Chun Chen ² 

¹ Department of Materials Science and Engineering, National Yang Ming Chiao Tung University, Hsinchu 30010, Taiwan; j73628.mse95g@nctu.edu.tw (K.-A.C.); dohienvl@gmail.com (T.-H.D.)

² National Applied Research Laboratories, Taiwan Instrument Research Institute, Hsinchu 30010, Taiwan; weichun@tiri.narl.org.tw

* Correspondence: z3aptx4869@yahoo.com.tw (C.-H.Y.); lichang@cc.nctu.edu.tw (L.C.); Tel.: +886-3-5712121 (ext. 55373) (L.C.); Fax: +886-3-5724727 (L.C.)

Abstract: Plasma nitridation of an amorphous SiO₂ layer on Si (110) substrate can form well-aligned α -Si₃N₄ crystallites in fibrous morphology. Nitriding is performed at a temperature in the range of 800–1000 °C by using microwave plasma with a gas mixture of N₂ and H₂. Raman spectroscopy shows the characteristics of an α -Si₃N₄ phase without other crystalline nitrides. As shown by scanning electron microscopy, the formed α -Si₃N₄ microfibers on the Si substrate can be in a dense and straight array nearly along with Si $\langle 1\bar{1}0 \rangle$, and can have a length over 2 mm with a diameter in the range of 5–10 μ m. Structural characterization of scanning transmission electron microscopy in cross section view reveals that the elongated α -Si₃N₄ crystallites are formed on the surface of the nitrided SiO₂/Si (110) substrate without any interlayers between Si₃N₄ and Si, and the longitudinal direction of α -Si₃N₄ appears mainly along $\langle 11\bar{2}0 \rangle$, which is approximately parallel to Si $\langle 1\bar{1}0 \rangle$.

Keywords: Si₃N₄; plasma; nitridation; fiber; electron microscopy



Citation: Yu, C.-H.; Chiu, K.-A.; Do, T.-H.; Chang, L.; Chen, W.-C.

Formation of Aligned α -Si₃N₄ Microfibers by Plasma Nitridation of Si (110) Substrate Coated with SiO₂. *Coatings* **2021**, *11*, 1251. <https://doi.org/10.3390/coatings11101251>

Academic Editor: Maria Vittoria Diamanti

Received: 18 August 2021
Accepted: 7 October 2021
Published: 14 October 2021

Publisher's Note: MDPI stays neutral with regard to jurisdictional claims in published maps and institutional affiliations.



Copyright: © 2021 by the authors. Licensee MDPI, Basel, Switzerland. This article is an open access article distributed under the terms and conditions of the Creative Commons Attribution (CC BY) license (<https://creativecommons.org/licenses/by/4.0/>).

1. Introduction

Silicon nitride (Si₃N₄) has been used in many structural applications for a long time due to its excellent properties, such as high hardness and high-temperature stability, resistance to thermal shock, and wear resistance. In addition, Si₃N₄ has a wide band gap ($E_g = 4.7$ eV) which can be applied for semiconductor devices [1,2]. Si₃N₄ has many different crystal structures, among which α -Si₃N₄, β -Si₃N₄, and γ -Si₃N₄ are common phases. Both α -Si₃N₄ and β -Si₃N₄ can be formed under ambient conditions at high temperatures, while γ -Si₃N₄ exists under high temperature and high pressure [3–5]. In addition, crystalline Si₃N₄ synthesis, generally in polycrystalline microstructure, has been widely conducted by nitridation of Si and SiO₂ powders at high temperature. Plasma nitriding has been proven to be effective for material synthesis [6–8]. Plasma nitridation of SiO₂ and Si for the formation of Si₃N₄ have been studied in previous reports by using thermal and radio frequency plasma processes with gases containing nitrogen [9–11] in which hydrogen may be necessary for the oxide reduction, and nitrogen reaction with Si formed nitride. It is well known that microwave plasma can easily achieve high plasma density which has been applied in various applications, including etching and film deposition. In our recent studies, we have shown that microwave plasma can be effectively applied for nitridation of *c*-plane and *m*-sapphires to form epitaxial AlN. In addition, epitaxial TiN can obtain plasma nitridation of rutile TiO₂ [12–14].

Various forms of crystalline Si₃N₄ have been synthesized, including whiskers and nanowires which may have potential applications in nanocomposites and electronic devices. Si₃N₄ nanowires have been synthesized by various methods, including chemical vapor deposition and nitridation [15–18]. Recently, we have used microwave plasma for nitridation of a SiO₂/Si (111) substrate to form {10 $\bar{1}0$ }-oriented crystalline α -Si₃N₄ and

β - Si_3N_4 which have elongated wire morphologies in lengths of several hundred micrometers and are mainly aligned with three different Si $\langle 110 \rangle$ directions [19]. In this study, the formation of crystalline Si_3N_4 on an Si (110) substrate which was coated with SiO_2 was investigated. Furthermore, we try to understand the role of Si orientation on the alignment of Si_3N_4 . The results showed that crystalline α - Si_3N_4 microfibers in aligned arrays with a length more than 2 mm are mainly formed along a *unique* direction of Si $\langle 1\bar{1}0 \rangle$ on Si (110).

2. Materials and Methods

In this work, a 50 nm thick SiO_2 film grown on a two inch Si (110) wafer was used as substrate. Growth of the SiO_2 film was performed at 300 °C by plasma-enhanced chemical vapor deposition using a gas mixture of SiH_4 , N_2O , and Ar. After the deposition of SiO_2 , the substrate was cut to pieces about $1 \times 1 \text{ cm}^2$. Nitridation of the SiO_2/Si (110) substrate with a gas mixture of N_2 and H_2 was performed in a microwave (2.45 GHz) plasma system, which was commonly employed for chemical vapor deposition of diamond [20,21]. The flow rate of N_2 and H_2 was 285 and 15 sccm, respectively. The microwave power was set at 700 W and a pressure of $5.3 \times 10^3 \text{ Pa}$. The nitridation was carried out for 10 and 20 min. The substrate temperature during plasma nitriding was estimated to be in the range of 800–1000 °C as measured by optical pyrometer (wavelength of 0.96 μm).

Raman spectroscopy was carried out in a Horiba Jobin Yvon LabRAM HR 800 spectrometer with 50 mW Ar laser ($\lambda = 533 \text{ nm}$). Scanning electron microscopy (SEM, JEOL JSM-6500F, Tokyo, Japan). was performed to examine surface morphologies of the SiO_2/Si (110) substrates. Cross-sectional scanning transmission electron microscopy (ARM200F, JEOL, Tokyo, Japan) with high-resolution transmission electron microscopy (HRTEM) was performed for crystallographic evaluation. Cross-sectional STEM specimen preparation was performed in a dual-beam focused ion beam (FIB, TESCAN LYRA3) system. Before FIB cutting, a 50 nm thin layer of amorphous carbon (a-C) and a 240 nm layer of platinum (Pt) were deposited on the nitride sample surface with an electron beam, followed by deposition of a 250 nm layer of a-C and a 300 nm layer of Pt with ion beam as protective coating.

3. Results

Figure 1a shows a typical SEM micrograph of the nitrided SiO_2/Si (110) substrate after 10 min nitriding. The surface morphology shows that Si_3N_4 crystallites exhibit a fiber-like characteristic with an average diameter of about 1–2 μm and a length of $>0.1 \text{ mm}$. Those Si_3N_4 microfibers are predominately aligned in parallel with each other and approximately along the specific direction of Si $[1\bar{1}0]$. For 20 min nitridation, the length of the microfibers can be as long as 2 mm and the diameter can increase to 5–10 μm , as shown in Figure 1b,c. A few areas on the nitrided substrate are covered with highly dense microfibers. The microfibers shown in Figure 1c exhibit a prism-like morphology, and most of the microfibers are aligned nearly with their longitudinal directions Si $[1\bar{1}0]$ in addition to a few deviated ones. The faceted morphology suggests that the microfibers are of the crystalline phase. Furthermore, X-ray energy dispersive spectroscopy shows that those microfibers consist of Si and N, as shown in Figure 1d, with the absence of O, implying that SiO_2 may not exist anymore after nitriding.

Raman spectra from different areas on the SEM images shown in Figure 1 were acquired in micromode. A typical Raman spectrum acquired from the microfibers is shown in Figure 2 from 150 to 450 cm^{-1} . The Raman peaks observed at 259 and 363 cm^{-1} are identified to belong to α - Si_3N_4 [22]. The Raman peak at 300 cm^{-1} is the characteristic signal of Si in second order [23,24]. As no β - Si_3N_4 characteristic peaks are observed, it is evident that all the microfibers are of the α - Si_3N_4 phase. On the bare area without coverage of the Si_3N_4 crystallites as shown in Figure 1b, neither Si_3N_4 nor SiO_2 Raman signals can be observed, implying that SiO_2 after nitridation might transform to Si_3N_4 , or be etched away by the plasma containing hydrogen. Many of the glass vibrations are

known to occur between $400\text{--}700\text{ cm}^{-1}$ (bridging Si-O-Si vibrations) which are not seen in the spectrum [24].

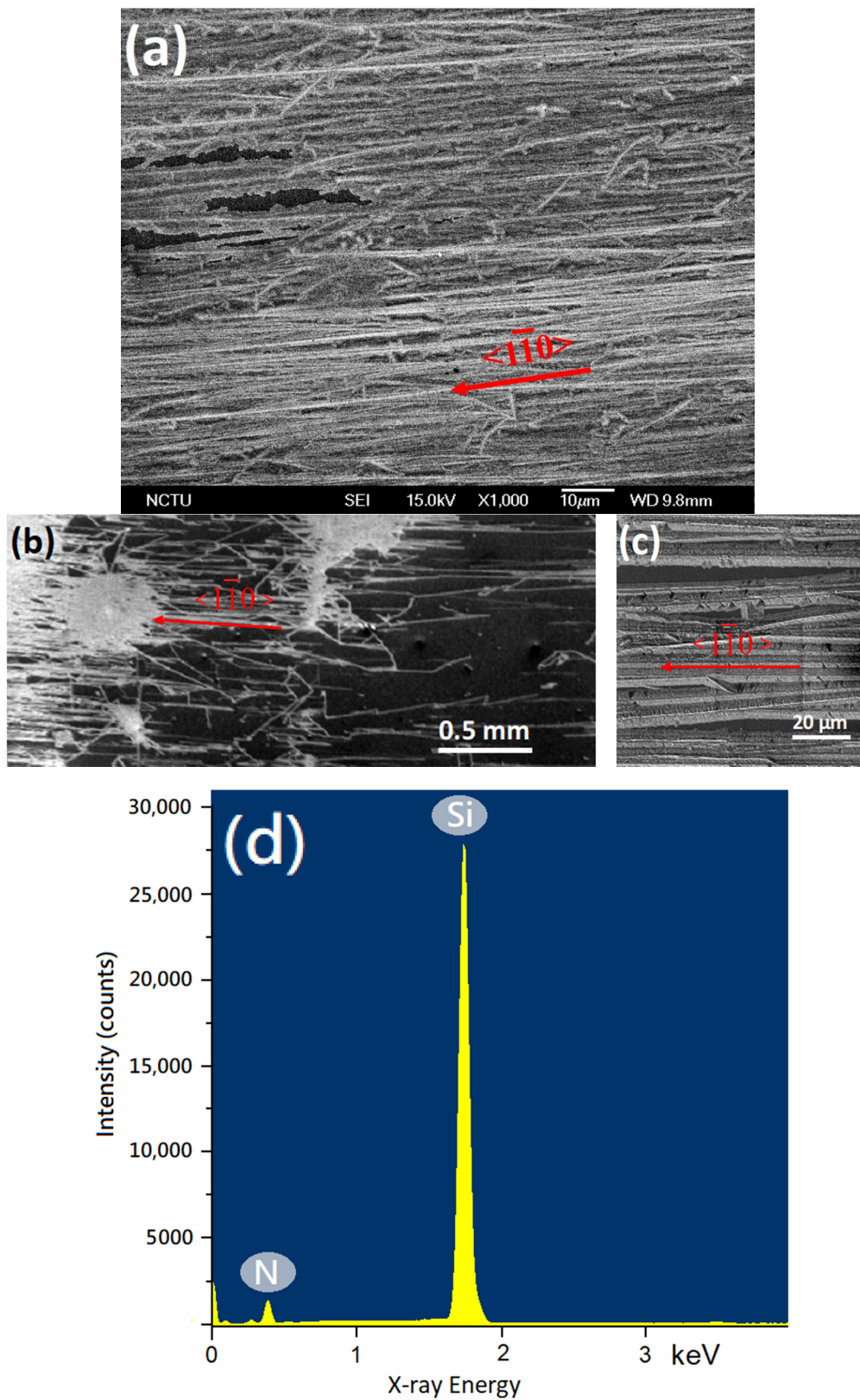


Figure 1. SEM surface morphology after nitriding for (a) 10 min and (b) 20 min. (c) Enlarged view of a dense region. (d) EDS spectrum of microfibers.

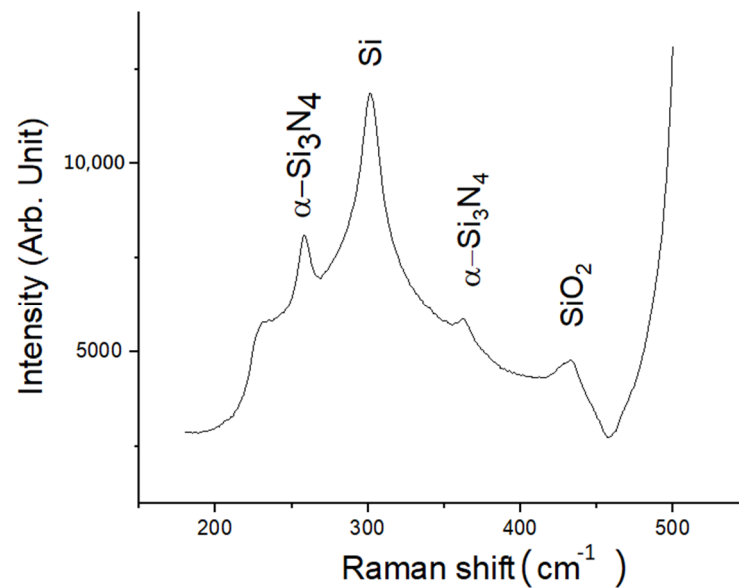


Figure 2. Raman spectrum of a nitrated substrate of SiO₂/Si after nitriding for 20 min.

Figure 3 shows typical cross-sectional TEM/STEM images from the nitrated sample for 20 min nitridation after tilting about 7° away from the Si [1 $\bar{1}$ 0] zone axis with the edge-on orientation for the Si₃N₄/Si interface. Figure 3a,b show low-magnification annular bright field (ABF) and annular dark field (ADF) images in diffraction and atomic number contrast, respectively. As can be seen, the Si₃N₄ thickness is varied from 70 to 270 nm, and no interlayers exist between Si₃N₄ and Si. Figure 3c shows a typical high-resolution TEM (HRTEM) image taken from the central region in Figure 3a where the thickness is about 270 nm after tilting about 2° away from the Si [1 $\bar{1}$ 0] zone axis to align Si₃N₄ in [2 $\bar{1}$ $\bar{1}$ 0] the zone axis. The HRTEM image shows that Si₃N₄ is in direct contact with Si though the interface between them is not flat. The corresponding fast Fourier transform (FFT) pattern from Si₃N₄ shown in the upper inset demonstrates that Si₃N₄ is an α -phase in [2 $\bar{1}$ $\bar{1}$ 0] the zone axis, whereas the Si FFT pattern shown in the lower inset is deviated from the [1 $\bar{1}$ 0] zone axis. Nevertheless, it can still recognize the pattern characteristics of Si with those reflections to understand the essential orientations with respect to Si₃N₄ ones. Furthermore, an atomic resolution ADF STEM image, as shown in Figure 3d, with the corresponding FFT pattern of Si₃N₄ in [2 $\bar{1}$ $\bar{1}$ 0] zone axis reveals detailed information at the interface where the Si₃N₄ lattice can have a reasonably good match with the Si one, i.e., {10 $\bar{1}$ 0} interplanar spacing of 0.672 nm is correspondingly matched with two Si {111} ones of 0.628 nm, implying that there may exist a specific orientation relationship between Si₃N₄ with Si. In addition, it is seen that the zone axis of α -Si₃N₄ [2 $\bar{1}$ $\bar{1}$ 0] is approximately parallel to Si [1 $\bar{1}$ 0] with about 2° deviation, suggesting that the lattice mismatch along such a direction is small. The small lattice mismatch can be understood as α -Si₃N₄ has lattice parameter $a = 7.765 \text{ \AA}$ in [2 $\bar{1}$ $\bar{1}$ 0], and the magnitude of the Si [1 $\bar{1}$ 0] direction is 7.681 \AA . Linear fits yield the Young's modulus, $E = 339 \text{ GPa}$, and the Poisson's ratio, $\nu = 0.32$ [25].

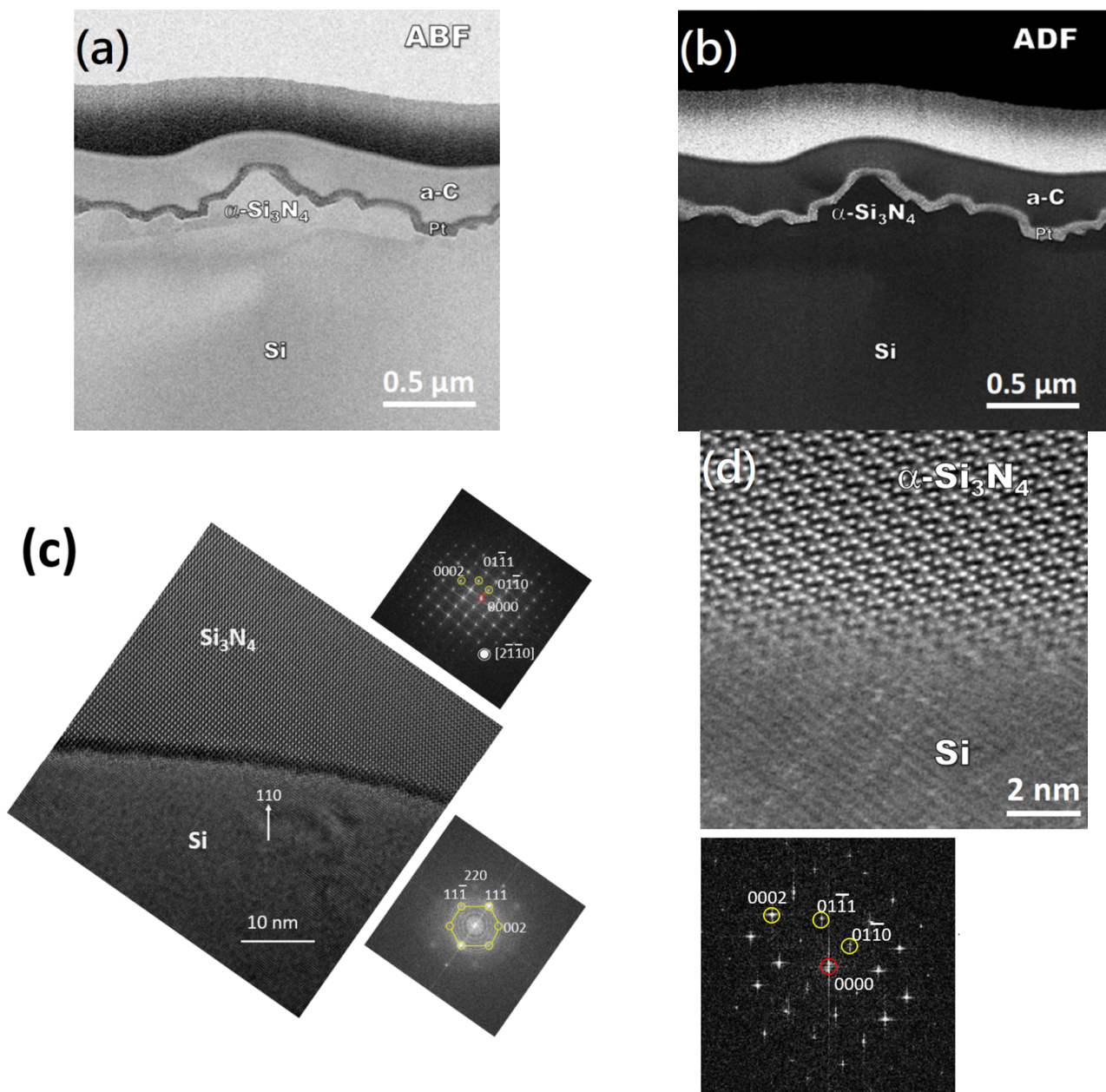


Figure 3. (a,b) Low magnification cross-sectional STEM–ABF and ADF images of α -Si₃N₄ on Si, respectively; (c) HRTEM image of the Si₃N₄/Si interface from the central region in (a) with the corresponding FFT patterns of α -Si₃N₄ and Si; (d) Atomic resolution STEM-ADF image of the α -Si₃N₄/Si interface with the corresponding FFT pattern of α -Si₃N₄ in zone axis [1120].

4. Discussion

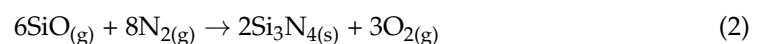
From the above results, a number of issues on Si₃N₄ formation will be discussed, including orientation and phase on Si substrate (110) versus (111) the role of SiO₂, plasma condition for nitridation, and fiber morphology.

Though Raman spectra and TEM examinations clearly show the formation of crystalline α -Si₃N₄, no Si₃N₄ diffraction peaks from the samples can be observed in acquired θ -2 θ X-ray diffraction (XRD) patterns in the range of 10–90°, implying that those microfibers are in a large inclined angle away from those diffraction reflections of low indices, such as 1010, 1011, 1120, 2021, and 0002. From the FFT patterns of α -Si₃N₄ in Figure 3, 1011 reflection is deviated about 7° from the Si surface normal, such that its diffraction signal could not be detected in general θ -2 θ XRD scan.

It is known that α -to- β transformation takes place at high temperatures (~ 1900 °C) and the process is irreversible. It has been shown that β - Si_3N_4 is thermodynamically more stable than α - Si_3N_4 up to 2000 K [26], and α - Si_3N_4 is a metastable phase under ordinary pressure. However, plasma nitridation can be considered as a nonequilibrium condition to form α - Si_3N_4 . Therefore, it might be the dominant phase for the short time of nitridation. Currently, it is not known why the formation of only α - Si_3N_4 occurs on Si (110), while both α - and β phases are formed on Si (111), even if the surface energy of Si (110) is higher than Si (111), which might lead to a lower energy barrier for α - Si_3N_4 nucleation [27]. However, it is worth pointing out that most of previous studies on nitridation for formation of Si_3N_4 nanowires and fibers show only an α -phase formed [15,28].

Direct nitridation of bare Si substrate without SiO_2 under the same plasma condition for 20 min shows no nitride formation, as no Raman signals can be observed and SEM observations show that the surface of the Si substrate remains to be as smooth as that before nitridation. Si_3N_4 formation is slow for nitridation of Si and the thickness formed is only a few nanometers after long-time nitriding, while the nitridation rate is faster with SiO_2 to form a thicker nitride film [29]. Thus, it is likely that the reaction of Si with N from the plasma will be retarded with the presence of H in plasma, and it might require an extended period of plasma nitridation to obtain Si_3N_4 .

For thermal nitridation, Si and SiO_2 can react to form SiO gas species which then react with nitrogen for nitride formation as the following reactions of (1) and (2) [30].



It has been reported that silicon oxide can be nitrated easily below 700 °C using nitrogen plasma generated by electron impact and a large amount of nitrogen can be incorporated in the oxide [5,31]. As most of the gas phases for nitridation can be effectively decomposed in the microwave plasma, there may be plenty of atoms, radicals, and ions as reactive species which can be available for the reactions on the substrate surface. The chemical reactions might occur with a faster rate under the microwave plasma condition. In addition, microwave plasma with H can effectively reduce SiO_2 to Si which then reacts with N. In particular, atomic hydrogen may play a critical role on nitridation. The diffusion rate of atomic hydrogen from the plasma might be faster than that of nitrogen toward the SiO_2 /Si interface to delaminate the oxide layer, whereas hydrogen can reduce the oxide surface to expose the bare Si surface which may have a slow reaction with N in comparison with the SiO reaction with N to form Si_3N_4 [32,33]. The accelerated nitriding rates due to the interaction of hydrogen with native oxide on the surface of the Si particles were observed in previous studies [34,35]. Similarly, SiO_2 can be transformed to Si_3N_4 by N_2/H_2 microwave plasma in the present case. In addition, it can be seen that pure N_2 plasma nitridation of SiO_2 may result in the formation of SiON instead of Si_3N_4 .

Nitridation of Si (110) has been previously investigated. Saranin et al. reported that the Si(110) surface after thermal nitridation by NH_3 gas in the temperature range of 560–1050 °C is covered with epitaxial islands of Si-nitride in a thickness less than 1 nm, followed by layer-by-layer growth [36]. Higuchi et al. also reported that high-quality Si_3N_4 film in a thickness < 5 nm was formed by nitridation of the Si(110) surface at 600 °C using radical NH [5]. Also, nitridation of Si(110) under RF plasma and the thermal process forms a very thin ($10\bar{1}1$) α - Si_3N_4 epitaxial layer [37]. In contrast, the present work shows that on Si (110), the α - Si_3N_4 microfibers only align along with the single direction of Si [$1\bar{1}0$] after nitridation by microwave plasma. Though the exact mechanism for α - Si_3N_4 formation is not currently known, it may be of interest to understand the relationship from the crystallography point of view. While SiO_2 can be decomposed by N_2/H_2 plasma, the nucleation and growth of Si_3N_4 could be fast along Si <110> due to low strain energy from the small lattice mismatch between them along Si <110> and Si_3N_4 <1120>.

Nitridation of Si and SiO₂ to form nanowires and nanofibers were previously reported. Ramesh and Rao reported formation of α -Si₃N₄ fibers by carbothermal reduction and nitridation reaction of SiO₂ with N₂ gas at 1623K [38]. Also, a few reports have shown synthesis of α -Si₃N₄ nanowires by nitriding nanocrystalline Si powder at 1300 °C for 2 h in pure N₂ [39]. Kim et al. demonstrated synthesis of silicon nitride nanowires directly from the silicon substrates via a catalytic reaction under ammonia or hydrogen flow at 1200 °C, using Ga, GaN, and Fe nanoparticles as catalysts [29]. However, those nanowires are randomly distributed. Formation of α -Si₃N₄ whiskers by nitridation have been also reported by previous studies [35,40,41]. The synthesis of Si₃N₄ nanowires from the reaction of Si nanoparticles with N₂ in the temperature range of 1200–1440 °C is also reported [42–44]. Ordered arrays of α -Si₃N₄ nanowires have been also synthesized at 1150 °C with NH₃ [45,46]. Direct synthesis of α -Si₃N₄ nanowires from silicon monoxide on alumina with N₂/H₂ was also reported [47]. Similarly, it has been demonstrated that single-crystalline α -Si₃N₄ nanowires can grow in a direction perpendicular to the wet-etched trenches in the SiO film on the plane of the Si substrate without metal catalysis [33].

5. Conclusions

Microwave plasma nitriding of 50 nm SiO₂ on Si(110) substrate using a gas mixture of H₂ and N₂ can form aligned microfibers of crystalline α -Si₃N₄ nearly along with Si [1 $\bar{1}$ 0]. The formed Si₃N₄ microfibers can have a length as long as 2 mm with a diameter of 5–10 μ m. Cross-sectional STEM examinations reveal that Si₃N₄ directly forms on Si without any residual SiO₂ after nitriding. Furthermore, it is shown that most of the microfibers have their longitudinal direction along Si₃N₄ <11 $\bar{2}$ 0>, which is approximately parallel to Si [1 $\bar{1}$ 0].

Author Contributions: Conceptualization, C.-H.Y. and L.C.; Data curation, C.-H.Y., K.-A.C. and W.-C.C.; Formal analysis, C.-H.Y., T.-H.D. and K.-A.C.; Funding Acquisition, W.-C.C. and L.C.; Methodology, C.-H.Y.; Software, T.-H.D.; Supervision, L.C.; Validation, C.-H.Y.; Writing—original draft, C.-H.Y.; Writing—review & editing, L.C. All authors have read and agreed to the published version of the manuscript.

Funding: This work was supported by Ministry of Science and Technology, Taiwan, R.O.C. under contract of MOST 107-2221-E-009-009-MY2.

Institutional Review Board Statement: Not applicable.

Informed Consent Statement: Not applicable.

Data Availability Statement: Data sharing is not applicable to this article.

Conflicts of Interest: The authors declare no conflict of interest.

References

1. Unal, O.; Petrovic, J.; Mitchell, T. CVD Si₃N₄ on single crystal SiC: Part I. Characterization and orientation relationship at the interface. *J. Mater. Res.* **1992**, *7*, 136–147. [[CrossRef](#)]
2. Kim, J.W.; Yeom, H.W. Surface and interface structures of epitaxial silicon nitride on Si(111). *Phys. Rev. B* **2003**, *67*, 035304. [[CrossRef](#)]
3. Riley, F.L. Silicon Nitride and Related Materials. *J. Am. Ceram. Soc.* **2004**, *83*, 245–265. [[CrossRef](#)]
4. Murakawa, S.; Ishizuka, S.-I.; Nakanishi, T.; Suwa, T.; Teramoto, A.; Sugawa, S.; Hattori, T.; Ohmi, T. Depth Profile of Nitrogen Atoms in Silicon Oxynitride Films Formed by Low-Electron-Temperature Microwave Plasma Nitridation. *Jpn. J. Appl. Phys.* **2010**, *49*, 091301. [[CrossRef](#)]
5. Higuchi, M.; Aratani, T.; Hamada, T.; Shinagawa, S.; Nohira, H.; Ikenaga, E.; Teramoto, A.; Hattori, T.; Sugawa, S.; Ohmi, T. Electric Characteristics of Si₃N₄ Films Formed by Directly Radical Nitridation on Si(110) and Si(100) Surfaces. *Jpn. J. Appl. Phys.* **2007**, *46*, 1895–1898. [[CrossRef](#)]
6. Seino, T.; Matsuura, T.; Murota, J. Atomic-order nitridation of SiO₂ by nitrogen plasma. *Surf. Interface Anal.* **2002**, *34*, 451–455. [[CrossRef](#)]
7. Sahu, B.B.; Yin, Y.; Han, J.G. Effect of plasma parameters on characteristics of silicon nitride film deposited by single and dual frequency plasma enhanced chemical vapor deposition. *Phys. Plasmas* **2016**, *23*, 033512. [[CrossRef](#)]

8. Lee, E.L.; Wachs, I.E. In Situ Raman Spectroscopy of SiO₂-Supported Transition Metal Oxide Catalysts: An Isotopic ¹⁸O–¹⁶O Exchange Study. *J. Phys. Chem. C* **2008**, *112*, 6487–6498. [[CrossRef](#)]
9. Unal, O.; Mitchell, T. CVD Si₃N₄ on single crystal SiC: Part II. High resolution electron microscopy and atomic models of the interface. *J. Mater. Res.* **1992**, *7*, 1445–1454. [[CrossRef](#)]
10. Malvos, H.; Michel, H.; Ricard, A. Correlations between active species density and iron nitride layer growth in Ar-N₂-H₂ microwave post-discharges. *J. Phys. D Appl. Phys.* **1994**, *27*, 1328–1332. [[CrossRef](#)]
11. Tatarova, E.; Dias, F.; Gordiets, B.; Ferreira, C. Molecular dissociation in N₂-H₂ microwave discharges. *Plasma Sources Sci. Technol.* **2004**, *14*, 19–31. [[CrossRef](#)]
12. Ma, Z.-C.; Chiu, K.-A.; Wei, L.-L.; Chang, L. Formation of m-plane AlN on plasma-nitrided m-plane sapphire. *Jpn. J. Appl. Phys.* **2019**, *58*, SC1033. [[CrossRef](#)]
13. Chen, Y.-C.; Chang, L. Epitaxial AlN on c-plane sapphire by plasma nitriding. *Jpn. J. Appl. Phys.* **2019**, *58*, SC1012. [[CrossRef](#)]
14. Do, T.H.; Chang, C.; Wei, L.-L.; Chiu, K.-A.; Chang, L. Epitaxial TiN formation on rutile titanium dioxide (0 0 1) single crystal by nitridation. *Appl. Surf. Sci.* **2019**, *506*, 144614. [[CrossRef](#)]
15. Lin, L.W.; He, Y.H. Synthesis and optical property of ultra-long alpha-Si₃N₄ nanowires under superatmospheric pressure conditions. *CrystEngComm* **2012**, *14*, 3250–3256. [[CrossRef](#)]
16. Gao, F.; Yang, W.; Fan, Y.; An, L. Aligned ultra-long single-crystalline α-Si₃N₄ nanowires. *Nanotechnology* **2008**, *19*, 105602. [[CrossRef](#)]
17. Dong, S.; Hu, P.; Zhang, X.; Cheng, Y.; Fang, C.; Xu, J.; Chen, G. Facile synthesis of silicon nitride nanowires with flexible mechanical properties and with diameters controlled by flow rate. *Sci. Rep.* **2017**, *7*, 45538. [[CrossRef](#)]
18. Wang, X.; Wang, H.; Jian, K. Synthesis and formation mechanism of α-Si₃N₄ single-crystalline nanowires via direct nitridation of H₂-treated SiC fibres. *Ceram. Int.* **2018**, *44*, 12847–12852. [[CrossRef](#)]
19. Yu, C.-H.; Chiu, K.-A.; Do, T.-H.; Chang, L. Oriented Si₃N₄ crystallites formed by plasma nitriding of SiO₂/Si (111) substrate. *Surf. Coat. Technol.* **2020**, *395*, 125877. [[CrossRef](#)]
20. Truscott, B.S.; Kelly, M.W.; Potter, K.J.; Johnson, M.; Ashfold, M.N.R.; Mankelevich, Y.A. Microwave Plasma-Activated Chemical Vapor Deposition of Nitrogen-Doped Diamond. I. N₂/H₂ and NH₃/H₂ Plasmas. *J. Phys. Chem. A* **2015**, *119*, 12962–12976. [[CrossRef](#)]
21. Loureiro, J.; Ricard, A. Electron and vibrational kinetics in an N₂-H₂ glow discharge with application to surface processes. *J. Phys. D Appl. Phys.* **1993**, *26*, 163–176. [[CrossRef](#)]
22. Kuzuba, T.; Kijima, K.; Bando, Y. Raman-active modes of alpha silicon nitride. *J. Chem. Phys.* **1978**, *69*, 40. [[CrossRef](#)]
23. Faraci, G.; Mannino, G.; Pennisi, A.R.; Ruggeri, R.; Sberna, P.; Privitera, V. Raman and photoluminescence spectroscopy of Si nanocrystals: Evidence of a form factor. *J. Appl. Phys.* **2013**, *113*, 63518. [[CrossRef](#)]
24. Spizzirri, P.G.; Fang, J.-H.; Rubanov, S.; Gauja, E.; Prawer, S. Nano-Raman spectroscopy of silicon surfaces. *arXiv* **2010**, arXiv:1002.2692.
25. Swift, G.A.; Ustundag, E.; Clausen, B.; Bourke, M.A.M.; Lin, H.-T. High-temperature elastic properties of in situ-reinforced Si₃N₄. *Appl. Phys. Lett.* **2003**, *82*, 1039. [[CrossRef](#)]
26. Kuwabara, A.; Matsunaga, K.; Tanaka, I. Lattice dynamics and thermodynamical properties of silicon nitride polymorphs. *Phys. Rev. B* **2008**, *78*, 064104. [[CrossRef](#)]
27. Messmer, C.; Bilello, J.C. The surface energy of Si, GaAs, and GaP. *J. Appl. Phys.* **1981**, *52*, 4623–4629. [[CrossRef](#)]
28. Kim, H.Y.; Park, J.; Yang, H. Synthesis of silicon nitride nanowires directly from the silicon substrates. *Chem. Phys. Lett.* **2003**, *372*, 269–274. [[CrossRef](#)]
29. Hayafuji, Y.; Kajiwara, K. Nitridation of Silicon and Oxidized-Silicon. *J. Electrochem. Soc.* **1982**, *129*, 2102–2108. [[CrossRef](#)]
30. Zhang, Y.; Wang, N.; He, R.; Liu, J.; Zhang, X.; Zhu, J. A simple method to synthesize Si₃N₄ and SiO₂ nanowires from Si or Si/SiO₂ mixture. *J. Cryst. Growth* **2001**, *233*, 803–808. [[CrossRef](#)]
31. Kobayashi, H.; Mizokuro, T.; Nakato, Y.; Yoneda, K.; Todokoro, Y. Nitridation of silicon oxide layers by nitrogen plasma generated by low energy electron impact. *Appl. Phys. Lett.* **1997**, *71*, 1978–1980. [[CrossRef](#)]
32. Manjunatha, K.N.; Paul, S. Stability study: Transparent conducting oxides in chemically reactive plasmas. *Appl. Surf. Sci.* **2017**, *424*, 316–323. [[CrossRef](#)]
33. Wang, X.; Liu, J.; Cheng, B.; Yu, J.; Wang, Q. Metal catalysis-free, direction-controlled planar growth of single-crystalline α-Si₃N₄ nanowires on Si(100) substrate. *Nanotechnology* **2006**, *17*, 3989–3993. [[CrossRef](#)]
34. Dervišbegović, H.; Riley, F.L. The role of hydrogen in the nitridation of silicon powder compacts. *J. Mater. Sci.* **1981**, *16*, 1945–1955. [[CrossRef](#)]
35. Rahman, I.A.; Riley, F.L. The control of morphology in silicon nitride powder prepared from rice husk. *J. Eur. Ceram. Soc.* **1989**, *5*, 11–22. [[CrossRef](#)]
36. Saranin, A.; Tarasova, O.; Kotljar, V.; Khramtsova, E.; Lifshits, V. Thermal nitridation of the Si(110) by NH₃: LEED and AES study. *Surf. Sci.* **1995**, *331–333*, 458–463. [[CrossRef](#)]
37. Atanassova, E.D.; Popova, L.I. Plasma nitridation of thin SiO₂ films: AES, ELS and IR study. *J. Nucl. Mater.* **1993**, *200*, 421–425. [[CrossRef](#)]
38. Ramesh, P.D.; Rao, K.J. Carbothermal reduction and nitridation reaction of SiO_x and preoxidized SiO_x: Formation of α-Si₃N₄ fibers. *J. Mater. Res.* **1994**, *9*, 2330–2340. [[CrossRef](#)]

39. Wang, Q.; Cong, R.; Li, M.; Zhang, J.; Cui, Q. A simple method to synthesize α -Si₃N₄, β -SiC and SiO₂ nanowires by carbothermal route. *J. Cryst. Growth* **2010**, *312*, 2133–2136. [[CrossRef](#)]
40. Gedevanishvili, S.; Cherian, K.; Agrawal, D.; Roy, R. Synthesis of Silicon Nitride Whiskers by Microwave Heating. *MRS Proc.* **1998**, *547*, 13. [[CrossRef](#)]
41. Chen, F.; Li, Y.; Liu, W.; Shen, Q.; Zhang, L.; Jiang, Q.; Lavernia, E.J.; Schoenung, J.M. Synthesis of α silicon nitride single-crystalline nanowires by nitriding cryomilled nanocrystalline silicon powder. *Scr. Mater.* **2009**, *60*, 737–740. [[CrossRef](#)]
42. Farjas, J.; Pinyol, A.; Rath, C.; Roura, P.; Bertran, E. Kinetic study of the oxide-assisted catalyst-free synthesis of silicon nitride nanowires. *Phys. Status Solidi* **2006**, *203*, 1307–1312. [[CrossRef](#)]
43. Wang, F.; Qin, X.; Yang, L.; Meng, Y.; Sun, L. Synthesis and photoluminescence of Si₃N₄ nanowires from La/SiO₂ composites and Si powders. *Ceram. Int.* **2015**, *41*, 1505–1510. [[CrossRef](#)]
44. Tian, Z.; Chen, K.; Sun, S.; Zhang, J.; Cui, W.; Xie, Z.; Liu, G. Synthesis of Si₃N₄ nanowires by catalyst-free nitridation of (Si + SiO₂) mixture. *Micro Nano Lett.* **2019**, *14*, 919–921. [[CrossRef](#)]
45. Ahmad, M.; Zhao, J.; Zhang, F.; Pan, C.; Zhu, J. One-step synthesis route of the aligned and non-aligned single crystalline α -Si₃N₄ nanowires. *Sci. China Ser. E Technol. Sci.* **2009**, *52*, 1–5. [[CrossRef](#)]
46. Ahmad, M.; Zhao, J.; Pan, C.; Zhu, J. Ordered arrays of high-quality single-crystalline α -Si₃N₄ nanowires: Synthesis, properties and applications. *J. Cryst. Growth* **2009**, *311*, 4486–4490. [[CrossRef](#)]
47. Cui, J.; Li, B.; Zou, C.; Zhang, C.; Wang, S. Direct Synthesis of α -Silicon Nitride Nanowires from Silicon Monoxide on Alumina. *Nanomater. Nanotechnol.* **2015**, *5*, 32. [[CrossRef](#)]